

1 **Response to Editor**

2 On top of the comments made by the referees, I also have a suggestion in combination with Fig. 7 which
3 shows the synthetic and a field acquired hemispherical photograph. Since this figure shows qualitatively
4 the sensitivity to small errors in the exact location, it would be beneficial to show the daily timeserie of
5 the pyranometer (as in Fig. 4) with the simulated timeseries of a couple of points surrounding the
6 pyranometer. This may show that points located 1 or 2 meters away from the pyranometer give
7 simulated solar radiation similar to the observed one.

8 WE HAVE ADDED A FIGURE 8 WHICH SHOWS THE PYRANOMETER TIMESERIES FOR FIGURE 7. THE
9 PREDICTED SOLAR RADIATION IS ACTUALLY VERY SIMILAR TO THE OBSERVED PYRANOMETER DATA (0.58
10 VS 0.55 VS 0.57 kW/m². IT WAS CHOSEN BECAUSE IT WAS PARTICULARLY EASY TO OBSERVE HOW SMALL
11 LOCATION ERRORS COULD POTENTIALLY AFFECT THE SIMULATED SUNPATH. WE DO NOT HAVE A
12 METHODOLOGY TO SIMULATE A TIMESERIES, BUT WE ARE WILLING TO DO ADDITIONAL ANALYSES IF
13 YOU THINK THEY WOULD BE HELPFUL.

14

15 In stream temperature models it often does not matter that much if the exact location of solar
16 insolation is shifted a few meters.

17 Having said this, I was also wondering if you have taken into account that the pyranometer was located
18 1 m above the surface. Especially if solar angles are low, this may influence your result.

19 THE HEMISPHERICAL PHOTOGRAPH AND PYRANOMETER WERE TAKEN AT THE SAME HEIGHT, BUT IT IS
20 A GOOD POINT THAT THE ADDITIONAL METER IS NOT PROPERLY ACCOUNTED FOR IN COMPARING
21 LIDRA AND THE FIELD METHODS. WE WILL ADD LANGUAGE POINTING OUT THIS COULD BE A SOURCE
22 OF ERROR.

23 **Response to Reviewer 1**

24

25 On three substantive issues I have concerns: Model vs predictor. The abstract clearly states this paper is
26 testing two models with two validation datasets. However, under Model Comparisons, the discussion
27 changes to four "predictors" without explanation how these relate to the two models or why effective
28 leaf area index is included, as it is part of neither model. This confusion is compounded under Model
29 Application, where the predictors are now referred to as Model G and Model E, in reference to graphs in
30 figure 6. More consistent naming from methods through the discussion would make this easier to
31 follow.

32 AGREED THAT THIS IS CONFUSING AND IMPRECISE. THE FINAL VERSION WILL BE EDITED TO CLARIFY THE
33 EXACT PREDICTORS USED IN THE ABSTRACT, METHODS, RESULTS AND DISCUSSION.

Formatted: Font: Bold

34 Pyranometer validation. The spectral response of silicon-cell photodiodes is calibrated to clear sky
35 direct sunlight conditions, because it is not sensitive to the full shortwave spectrum and responds to
36 various wavelengths with different intensities. Leaf shading selectively blocks certain wavelengths,
37 which causes silicon pyranometers to decalibrate. Apogee estimates that this produces roughly a 19%
38 error under conifer canopy (<https://www.apogeeinstruments.com/content/SP-100-200-specsheet.pdf>,
39 page 15). Black body thermopile pyranometers are recommended for subcanopy light measurements.
40 They have an even spectral response across the shortwave spectrum even under leaves. I recommend
41 the authors acknowledge this as a source of uncertainty in their discussion.

42 THANK YOU FOR POINTING THIS OUT. WE WILL ADD THIS SOURCE OF UNCERTAINTY TO THE
43 DISCUSSION.

44 Conclusions. Line 256 "While both the raster-based LPI approach and the lidar point reprojection
45 synthetic hemispherical photograph approach achieve satisfactory model performance, the limited
46 range of solar insolation conditions at the point locations in our study limits some of the conclusions
47 that an be drawn." While I appreciate this study and the intent behind it, perhaps more validation data
48 is needed? Was there insufficient information to effectively evaluate the two models? How are both
49 approaches satisfactory

50

51 AGREED THAT "SATISFACTORY" IS NOT WELL-DEFINED AND THUS THIS STATEMENT IS NOT VERY
52 USEFUL. WILL REWORD TO INDICATE THAT THE RESULTS MAY BE SATISFACTORY DEPENDING ON THE
53 APPLICATION BUT MORE VALIDATION DATA IS NEEDED.

54

55 SPECIFIC COMMENTS

56 Line 146: The dates are not given for when the pyranometers were recorded. This makes a significant
57 difference for the models. On June 20, summer solstice, the shifted LPI and general LPI will look almost
58 identical, but December 20, winter solstice, will look radically different. Is there a reason this is not
59 mentioned, while the date for the Lidar is mentioned?

60 THIS WAS AN OVERSIGHT. PYRANOMETER AND HEMIPHOTO DATA WERE COLLECTED OVER TWO WEEKS
61 AROUND THE SUMMER SOLSTICE IN 2015. THIS INFORMATION WILL BE ADDED TO THE METHODS.

62 Line 251: Table 3 linear regression slope and intercept. I think this can be removed without loss to the
63 paper.

64 THIS IS INCLUDED FOR COMPLETENESS SAKE AND BECAUSE CERTAIN SCATTER PLOTS IN FIGURE 6 (eg. G
65 AND H MIGHT BE DIFFICULT TO INTERPRET WITHOUT THE INCLUSION OF A 1:1 LINE)

66 Line 269: Models should agree better in areas without shading. I am not sure how this is a conclusion.
67 While true, the whole point of these models is to tackle the uncertainty of heavily shaded landscapes.

68 THAT SENTENCE WILL BE REMOVED

69 Line 271: small registration errors. Recommend identifying which model this is an error for. Relevant for
70 synthetic photo, but not for raster.

71 AGREED. WILL INCLUDE IN REVISED VERSION

72 Line 281: understory vegetation. This is actually an argument against the directions this paper
73 recommends on Line 335 regarding ray tracing. Note the raster approach was developed with this issue
74 as one of the problems it was solving in its design.

75 GOOD OBSERVATION AND AGREED. WILL REMOVE RAY TRACING FROM THE CONCLUSION EXCEPT TO
76 NOTE THAT FURTHER RESEARCH IS NEEDED.

77 Line 294: "Model G and Model E (figure 6) performed the best..." This statement is unclear. How are
78 plots models? What criteria states that they performed the best? Their performance and the
79 performance of the hemispherical photos all seem within error of each other. Is this incorrect?

80 THIS CONCLUSION WAS BASED ON THE COEFFICIENT OF DETERMINATION. WE ARE CONSIDERING THE
81 SIMPLE LINEAR REGRESSION AS THE MODEL.

82 Line 337: "The results of this study suggest that refined ray-tracing approaches should not require
83 calibration." I do not see this statement supported by the paper. Both models used in this study did not
84 perform point cloud ray tracing. That is their strength. Musselman and Lee (referenced in introduction)
85 used voxel ray-tracing. Both required calibration.

86 AGREED. THIS SENTENCE WILL BE REMOVED AND RAY TRACING WILL BE REMOVED FROM CONCLUSION
87 EXCEPT FOR SHORT STATEMENT ON FURTHER RESEARCH.

88

89 RESPONSE TO REVIEWER 2

Formatted: Font: Bold

90 I appreciate very much that the authors provide their data and analysis (as is HESS standard now). While
91 I could easily follow the general setup of the study, I found it difficult to grasp the information residing in
92 the Lidar data set and how it has been used. Since the latter is not included in the repository: Did I
93 understand correctly that the Lidar data was commercially acquired and preprocessed to 1m pixels? So
94 each pixel has values about all point returns, the number of highest hits (canopy) and the number of
95 lowest hits (ground)?

96 THE LIDAR WAS PRE-PROCESSED BY THE VENDOR INTO 1 M PIXELS CONTAINING HIGHEST ELEVATION
97 AND GROUND MODEL. THE AUTHORS CREATED ADDITIONAL RASTERS USING THE RAW LIDAR POINTS IN
98 ORDER TO DETERMINE NUMBER OF CANOPY HITS AND GROUND HITS PER 1 M PIXEL

99 Please be more specific about the calculation methods than naming the Software ArcGIS. I suppose this
100 is an array operation which could be done in R (or any other math software) too. Which approaches did

101 you employ? What can be understood about the "10m Buffer around the field points" (L187) and how
102 does it differ to the "shifted square buffer" (L188f.)?

103 THESE CALCULATIONS COULD BE PERFORMED IN R OR ANY OTHER SOFTWARE BUT IT IS QUITE SIMPLE
104 TO DO IN ARCGIS. THE SPECIFIC OPERATIONS INCLUDED USING THE BUFFER TOOL AND SUMMING THE
105 NUMBER OF CANOPY AND GROUND POINTS QUANTIFIED IN THE VALUE FIELD OF THE RASTER USING
106 THE ZONAL STATISTICS TOOL. THE SHIFT CALCULATION WAS PERFORMED IN THE SAME WAY AFTER
107 USING THE EDITOR TOOL AND MOVE COMMAND TO SHIFT THE POINTS SOUTH BY 3.42 M. THE FINAL
108 VERSION WILL BE EDITED TO INCLUDE THIS SPECIFIC INFORMATION.

109 Did you average within this area for comparison?

110 WE SUMMED THE VALUES AS DESCRIBED ABOVE.

111 What are the effects on the performance of the estimates. Especially with regards to the issue of
112 "registration errors" L277ff. would this mean that a higher resolution could be more accurate or in other
113 words that the hemispherical photographs suffer from minor shading effects to become representative
114 at stand scale?

115 YES, THIS IS VALID CONCLUSION FROM THESE RESULTS.

116

117 For a validation of the Lidar-derived solar insolation there is basically the correlation plot in Fig. 8
118 comparing it to pyranometer measurements. To me this does not appear very convincing to support the
119 conclusion. By not allowing for an intercept in your linear regression model, you define the bias-term to
120 be zero. While this is an understandable desire in comparing two measurements which should give the
121 same results, I do not understand your statement in L298f.

122 AGREED THAT THIS IS NOT WELL STATED. THE INTENTION WAS TO BE ABLE TO PREDICT INSOLATION
123 WITH A MODEL THAT WOULD ESTIMATE INSOLATION TO BE ZERO IN AREAS WHERE NO CANOPY POINTS
124 WERE PRESENT. THIS WILL BE CLARIFIED IN REVISION

125

126 The 16 points appear to overestimate the pyranometer references in most cases. High insolation
127 references are underestimated. With an R2 of 0.63, I find it rather problematic to speak of accurate:
128 L329f. "a synthetic hemispherical photograph approach accurately predict solar insolation and light
129 transmittance".

130

131 WE STRUGGLE WITH DESIGNATING A THRESHOLD FOR ACCURACY, BUT AGREE THAT THIS IS NOT VERY
132 PRECISE TO DECLARE THIS ACCURATE WITHOUT A THRESHOLD. WILL REWORD TO SUGGEST THAT IT
133 MAY BE ACCURATE DEPENDING ON APPLICATION.

134 In this respect, I moreover have difficulties to relate this back to the presented indices which leaves me
135 with a couple of questions about the reason of their introduction in the first place. This confusion might
136 partially stem from the manifold usage of the term "model" in the manuscript. I would suggest to allow
137 for a more precise terminology to differentiate regression analyses from conversion models, from
138 indices and from spatial map models. From the title I was expecting several modelling approaches using
139 the Lidar data, which I did not find in the manuscript.

140 REVIEWER 1 HAD A SIMILAR CRITICISM AND WE WILL REVISE TO INDICATE WHAT WE MEAN BY MODEL.

141 Coming back to the indices (Fig. 6, Tab. 3) I do not find the focus of the study specifically suitable to
142 address these correlations.

143 YOUR CRITICISM IS NOT SUFFICIENTLY DETAILED FOR ME TO RESPOND IN DETAIL. I WILL SIMPLY SAY
144 THAT THE CORRELATIONS IN MY OPINION ARE SUITABLE AS THE OBJECTIVE OF THE STUDY IS TO
145 EVALUATE THE DIFFERENT METHODS COMPARED TO FIELD DATA.

146 Contrastingly, the comparison of synthetic and actual hemispherical photograph (Fig. 7) is very
147 compelling but falls in my view a little short in its analysis and evaluation (e.g. applying this for all 16
148 locations). Since the validation of the "Lidar-based modelling" is rather difficult using the 16
149 measurements alone, maybe some further reference could be derived from remote sensing products?
150 This could also provide the link to some of the addressed indices?

151 I'M NOT SURE WHAT SPECIFICALLY YOU ARE PROPOSING. WE ARE PRESENTING THIS WORK TO STAND
152 ALONE AND CANNOT AT THIS TIME EXPAND THE SCOPE.

153 2 Minor comments: L28f.: why only ecological applications?

154 THE SCOPE OF THIS STUDY IS FOCUSED ON ECOLOGICAL APPLICATIONS.

155 L29: do trees really interact (so having feedbacks) with solar radiation?

156 I WOULD ARGUE THAT TREES INTERACT WITH PHOTONS THROUGH REFLECTION, TRANSMITTANCE, AND
157 ABSORPTION. SHADING IS A COMBINATION OF THESE THREE EFFECTS.

158 L36: can (solar) energy intercept with something? maybe irradiate a stream?

159 WILL CHANGE TO IRRADIATE

160 L37: how does solar irradiation limit options for forest management? I do not understand.

161 THE REST OF THE PARAGRAPH EXPLAINS THIS, CULMINATING IN THE FINAL SENTENCE WHICH ANSWERS
162 YOUR QUESTION

163 L48ff.: is it really necessary to describe the function of a pyranometer (at this broad level of detail)?

164 I DON'T THINK IT DETRACTS FROM THE PAPER. SINCE THIS IS A HYDROLOGY JOURNAL I WANT THE
165 TECHNICAL INFORMATION TO BE WELL EXPLAINED.

166 L53: I do not see the difference between the time references of a direct state measurement and the
167 photograph

168 IT IS IN THE DIRECT VS INDIRECT MEASUREMENT. THE DIRECT MEASUREMENT IS DEPENDENT ON THE
169 ANGLE OF THE SUN WHILE THE INDIRECT MEASUREMENT IS NOT

170 L56: Depending on the type of pyranometer, diffuse radiation is directly measured too.

171 THIS IS REFERRING TO HEMISPHERICAL PHOTOGRAPHS

172 L67: Start new paragraph with "Airborne lidar..." ?

173 I SEE HOW IT COULD BE GOOD TO START A NEW PARAGRAPH THERE BUT THAT WOULD LEAD TO TWO
174 VERY SHORT PARAGRAPHS AND PREFER IT AS IS.

175 L113f.: very confusing. please rephrase.

176 I'M NOT SURE WHAT IS CONFUSING. THE CITATION TO THE ORIGINAL PAPER IS ALSO THERE TO HELP
177 READERS IF THEY ARE CONFUSED.

178 Fig 1: I would prefer all four Lidar models/maps instead of the grey box, which I assume to be the total
179 Lidar dataset footprint. If you find my suggestion feasible, maybe a map of a satellite RS derived index
180 could also be a reference here. A colourbar would be nice.

181 IT WOULD BE DIFFICULT TO FIT ALL FOUR MAPS IN THIS FIGURE WITHOUT MAKING THEM EXTREMELY
182 SMALL. THE GREY FOOTPRINT AND EXPLANATION OF THE COLORING IS IN THE CAPTION.

183 L200f.: What happened to the longitudinal profiles? Were they processed?

184 YES, THOSE ARE IN FIGURE 10.

185 L215: See general comment. Which exactly are THE models? do you refer to the different indices? the
186 calculus to derive them? a model to generate the synthetic hemispherical what are the assumptions
187 behind the comparison approach? What is the observation reference deemed as closest to the true
188 value?

189 SEE COMMENT ABOVE. WILL REVISE TO MAKE THIS MORE CLEAR.

190 L257: model performance? in reference to what? Is a R2 to each other really a good measure?

191 AGREED. IT IS A POINT THAT REVIEWER 1 ALSO BROUGHT UP AND WILL BE EDITED TO REMOVE
192 SATISFACTORY AND CLARIFY THAT R2 IS THE METHOD OF EVALUATION AND DISCUSS THE LIMITS OF THE
193 USE OF THAT STATISTIC.

194 L277ff.: I do not understand why this should not be desirable... actually, i find the results in fig 7 quite
195 convincing and the sensitivity ght be quite an interesting feature. Pls. see my general comment on this,
196 too.

197 IT IS UNDESIRABLE BECAUSE IT MAKES IT DIFFICULT TO EVALUATE THE ACCURACY OF THE MODELS. THIS
198 WILL HOPEFULLY BE MORE CLEAR WHEN THE MODEL LANGUAGE IS REVISED.

199

200 **RESPONSE TO REVIEWER 3**

Formatted: Font: Bold

201 The authors present an interesting study that compares two LiDAR based techniques (i.e., a raster-based
202 method and a synthetic hemispherical photograph approach) for estimating under canopy solar
203 insolation, which is an important variable for predicting stream temperature dynamics. They conduct
204 their study for sites on the heavily forested Panther Creek and its tributary located in Oregon, USA While
205 I am generally supportive of the merits of the study the authors present, I believe they could be more
206 precise in their language and provide more connecting details about the methods used so that their
207 work can be replicated and advanced. I also have some specific concerns about the methods in the
208 models. Additionally, throughout the paper, there is an emphasis on the ecological implications of this
209 work. However, stream temperature also has important implications for various biogeochemical
210 processes. The work the authors present may be of interest to other research domains so I would
211 recommend that the authors broaden their discussion to encompass them. I have provided some
212 general comments and suggestions that I hope the authors will consider incorporating into their paper
213 to address the problems I have enumerated.

214 General Comments 1. While the authors indicate that they used two LiDAR based approaches/models
215 for estimating solar insolation, midway through the paper, they introduce the new term “predictors”
216 and then switch back to models (Line 294). This is confusing. I would suggest that the authors select one
217 term and consistently use it throughout the paper. I would actually recommend sticking to predictor
218 since they are essentially correlating various shading surrogate indexes with measurements of solar
219 insolation. I also think it will be good introduce the specific predictors used under each approach (i.e.,
220 raster & synthetic hemispheric photograph approaches) at the beginning of the paper so that their
221 introduction later in the paper is not so abrupt. Under raster-based predictors they could introduce LPI,
222 SLPI, and LAI and then introduce %Transmittance for hemispheric photograph approach. They could also
223 discuss why they are good/suggested predictors for solar insolation citing references.

224 THIS IS SIMILAR TO COMMENTS MADE BY REVIEWER 1 AND 2. YOUR SPECIFIC RECOMMENDATIONS ARE
225 WELL RECEIVED AND WILL BE INCORPORATED INTO THE REVISED MANUSCRIPT.

226 2. The authors conclude that the limitation of their study was the lack of more monitoring points with
227 large insolation values and that inclusion of more of these points would have increased the model
228 accuracy (Line 266), but the point of their study was to derive approaches for estimating solar insolation
229 for streams with heavily forested riparian zones. This is in practice the areas where insolation estimation
230 uncertainty is greatest. My recommendation is to make this their focus and perhaps remove the points
231 with higher insolation values from their regression.

232 AGREE WITH THE GENERAL SENTIMENT OF THIS COMMENT. THE WORDING WAS INTENDED TO
233 INDICATE THAT IT WOULD HAVE BEEN EASY FOR US TO CHOOSE LOCATIONS WITH LOW CANOPY COVER

234 TO INCREASE THE ACCURACY OF THE MODEL, BUT THAT WOULD HAVE NOT BEEN PARTICULARLY
235 USEFUL. WE WILL REWORD THIS SECTION TO MAKE IT SEEM LESS LIKE A LIMITATION AND MORE A
236 RESULT THAT SHOULD STAND ON ITS OWN. NOTE THAT THE POINTS WITH HIGHEST %TRANSMITTANCE
237 ONLY HAD 35% SO WE DON'T THINK IT'S NECESSARY TO REMOVE THOSE AS THEY AREN'T
238 PARTICULARLY HIGH. WETHINK THE ISSUE IS MORE THAT WE WERE NOT ABLE TO CAPTURE ENOUGH
239 POINTS IN THE 15% TO 35% RANGE.

240 3. Throughout the paper, the authors use the word "significant" to describe differences between values
241 conjuring up an image of statistical significance. I would recommend that the authors state the actual
242 numerical differences or use other words.

243 AGREE AND THIS IS SIMILAR TO FEEDBACK GIVEN BY REVIEWER 1 AND 2.

244 4.

245 While the connection between solar insolation is self-apparent. I would recommend making that
246 connection more explicit in the paper. You could say something along the lines of "Solar radiation is a
247 major source heat flux into streams providing up to y% of heat fluxes" and the then cite a reference.

248 AGREE AND WILL ADD IN SIMILAR WORDING.

249 5. For the synthetic hemispherical photographs, what resolution was used for the hemisphere? Did it
250 match the field photographs? If different, what are the implications of the differences for the authors
251 analysis. I think the comparison of these too and the reasons why they might differ is an important
252 contribution.

253 IT'S A BIT DIFFICULT TO COMPARE AS THE SYNTHETIC PHOTOGRAPHS ARE CREATED USING POINTS THAT
254 ARE RENDERED WITH A RELATIVELY LARGE "DOT" SIZE COMPARED TO THE INDIVIDUAL PIXELS OF THE
255 CAMERA. THE "DOT" SIZE WAS DETERMINED BY THE MOESER ET AL (2014) ALGORITHM. THE INTENTION
256 IS FOR THE READER TO USE FIGURE 7 TO JUDGE THESE DIFFERENCES. WE ARE NOT SURE HOW
257 DIFFERENCES IN RESOLUTION WOULD AFFECT THE ANALYSIS.

258 Specific Comments 1. Line 16 – "due to the importance of temperature to aquatic biota". This makes it
259 sound like aquatic biota is the only reason why quantifying solar insolation is important. Consider
260 revising to broaden its implications.

261 IT WAS OUR MAIN MOTIVATION FOR EMBARKING ON THIS STUDY, BUT IT DOES LIMIT ITS
262 IMPLICATIONS. WILL CHANGE TO "USEFUL FOR A VARIETY OF APPLICATIONS, AND A SPECIFIC FOCUS OF
263 THIS STUDY IS THE IMPORTANCE OF STREAM TEMPERATURE TO AQUATIC BIOTA.

264 2. Line 17-19: I suggest changing "two approaches..." to something like "four predictor indexes
265 computed using two approaches for estimate shading effects from LiDAR" or something along these
266 lines. The larger point is that it is important to be precise in describing what was actually done.

267 AGREED. WE WILL MAKE THIS CHANGE.

268 3. Line 28 "is essential to a diversity of ecological. . ." Again, I think you can broaden this.
269 WILL ADD ANOTHER SENTENCE TO BROADEN THE SCOPE BEFORE FOCUSING ON ECOLOGICAL
270 APPLICATIONS.

271 4. Line 36 "solar energy intercepting a stream. . ." Consider revising to "solar energy irradiating a
272 stream"

273 SAME COMMENT WAS MADE BY REVIEWER 2 AND IT WILL BE CHANGED. 5.
274 Line 36-37 "can in turn limit options for forest management". Could the authors explain how increasing
275 temperatures limit options for forest management? I am not sure this is true.

276 A SIMILAR COMMENT WAS MADE BY REVIEWER 2. UPON FURTHER REFLECTION WE SEE HOW THIS
277 SENTENCE IS CONFUSING AND WILL EDIT IT TO MAKE THE CONNECTION BETWEEN STREAM
278 TEMPERATURES AND THE REQUIREMENT TO KEEP UNHARVESTABLE BUFFERS NEAR STREAMS

279 6. Line 45-46 "models may be needed..." I would argue that this is actually often the approach that is
280 used and is not a new insight so please consider revising to "models are therefore often employed to
281 estimate temperature"

282 GOOD POINT. WILL CHANGE TO ADOPT THAT LANGUAGE

283 7. Line 57: "solar output" consider revising to extra-terrestrial solar radiation.
284 WILL CHANGE. THANKS!

285 8. Line 60: "All ground-based. . ." Sounds a little too strong. Consider removing "All".
286 AGREED. WILL CHANGE

287 9. Line 78-79. "GIS software solar radiation calculators. . ." Consider revising to "Solar radiation
288 calculators in GIS software"

289 GOOD EDIT. WILL CHANGE.

290 10. Line 80-82. I think you are missing some words somewhere. Please rephrase for clarity. E.g., "r.sun
291 solar insolation model for the GRASS GIS software. . ."

292 AGREED THAT THIS IS PHRASED POORLY. WILL REWORD.

293 11. Line 89: What are Ellenburg indicator values? While ecologist might be familiar with them, I think it
294 will be good to explain.

295 WILL ADD A SHORT DESCRIPTION.

296 12. Line 169 Figure 4: Does the y axis name need to be solar irradiance for consistency? GOOD CATCH.
297 WILL CHANGE.

298 13. Line 195-197: I am not sure why this sentence is part of the paper. I feel it is unnecessary. Please
299 consider removing.

300 THE METHOD THAT WE USED BASED ON BODE ET AL (2014) USED THIS TOPOGRAPHIC CORRECTION
301 AND WE WANTED TO EXPLAIN WHY WE DID NOT FOLLOW THEIR METHOD COMPLETELY.

302 14. Line 198-199: Are the authors able to delve more into the details of the creation of these synthetic
303 photos?

304 THE CODE USED TO CREATE THESE WAS SHARED WITH PERMISSION BY DAVE MOESER AND WOULD
305 REFER YOU TO HIM FOR FURTHER DETAIL.

306 15. Line 222. "significantly improved" remove significantly for the reasons I raised earlier.

307 AGREED

308 16. Line 278: Please remove the word "significant". for the same reasons as before.

309 AGREED

310 17. Line 298-299: I am not sure I am comfortable removing the intercept and saying the resulting model
311 has little bias. By removing the intercept, the authors are making the R^2_{E2} value no longer useful.

312 THE INTERCEPT WAS REMOVED SO THAT PIXELS WITH NO CANOPY POINTS WOULD YIELD A PREDICTED
313 VALUE OF 0. WILL MAKE THIS REASONING EXPLICIT IN THE REVISED VERSION.

314 18. Line 311 & Figure 9: Please consider adding an inset that zooms to one of the monitoring points.

315 WE ARE NOT SURE WHAT YOU MEAN BY MONITORING POINTS. ARE YOU SUGGESTING AN INSET
316 SIMILAR TO FIGURE 1? IF SO, WE DON'T THINK A SIMILAR INSET WOULD BE PARTICULARLY USEFUL FOR
317 INTERPRETATION OF FIGURE

318 9. 19. Line 337-340: The authors pivots to ray tracing. However, the methods they use does not include
319 any ray tracing.

320 THIS POINT WAS BROUGHT UP BY REVIEWER 1 AND WE AGREE THAT IT DOES NOT BELONG. IT WILL BE
321 EDITED TO INCLUDE ONLY A SHORT REFERENCE TO RAY TRACING AS A POTENTIAL AVENUE OF FUTURE
322 RESEARCH

323

324

325

Formatted: Left

326 Lidar-based ~~modelling~~ approaches for estimating solar insolation in heavily forested streams

327

328 Richardson, Jeffrey J.*¹; Torgersen, Christian E.²; and Moskal, L. Monika³

329 ¹ Sterling College, Craftsbury Common, VT, USA

330 ²U.S. Geological Survey, Forest and Rangeland Ecosystem Science Center, Cascadia Field Station, University

331 of Washington, Seattle, WA, USA

332 ³ Precision Forestry Cooperative, School of Environmental and Forest Science, University of Washington,

333 Seattle, WA, USA

334 *Corresponding Author

335

336 ~~This draft manuscript is distributed solely for the purposes of scientific peer review. Its content is~~
337 ~~deliberative and predecisional, so it must not be disclosed or released by reviewers. Because the~~
338 ~~manuscript has not yet been approved for publication by the U.S. Geological Survey (USGS), it does not~~
339 ~~represent any official USGS finding or policy.~~

340 Abstract

341 Methods to quantify solar insolation in riparian landscapes are needed due to the importance of stream

342 temperature to aquatic biota. We have tested ~~two three lidar predictors using approachestwo~~

343 approaches developed for other applications of estimating solar insolation from airborne lidar using

344 field data collected in a heavily forested narrow stream in western Oregon, USA. We show that a raster

345 methodology based on the light penetration index (LPI) and a synthetic hemispherical photograph

346 approach both accurately predict solar insolation, explaining more than 73% of the variability observed
347 in pyranometers placed in the stream channel. We apply the LPI based model to predict solar insolation
348 for an entire riparian system, and demonstrate that no field-based calibration is necessary to produce
349 unbiased prediction of solar insolation using airborne lidar alone.

350 A. Introduction

351

352 Accurately quantifying solar insolation, defined as the amount of solar radiation incident on a specific
353 point on the Earth's surface for a given period of time, is important to many fields of study such as solar
354 energy, glacier dynamics, and climate modeling. In this study, we focus on the importance of solar
355 insolation for is-essential-to-a-diversity-of ecological applications. In forested ecosystems, trees interact
356 with solar radiation through shading, and thus solar insolation at fine spatial scales in these systems can
357 vary widely. Understanding the heterogeneous patterns of insolation below tree canopies has been
358 important for numerous applications, such as understanding the importance of sunflecks for understory
359 photosynthesis, gaining insight into the patterns of seedling regeneration in dense forests (Nicotra et al.,
360 1999), and explaining patterns of snowmelt (Hock, 2003) and soil moisture (Breshears et al., 1997).

361 The relationship between stream temperature and solar insolation is of particular interest in this study,
362 as high amounts of solar energy intercepting-irradiating a stream can cause adverse ecological effects
363 due to directly increasing the temperature of the streams.,-which can in turn limit options for forest
364 management near streams. In northwestern North America, a large amount of research has focused on
365 the relationship between forest practices, stream temperature, and the corresponding effect on river
366 salmonid fishes (Holtby, 1988;Leinenbach et al., 2013;Moore et al., 2005a;Moore et al., 2005b). Direct
367 measurement of stream temperature with in-stream thermographs can be used to quantify thermal
368 diversity (Torgersen et al., 2012;Torgersen et al., 2007), but ground-based measurements are time

369 consuming, expensive, and impractical for large areas. In addition, stream temperature measurements
370 can only show the effect of forest management practices if taken before and after trees are removed. In
371 order to predict the potential effect of forest management practices on stream temperature, models
372 ~~may are often employed to be needed to~~ estimate the amount of solar insolation
373 ~~intercepting irradiating~~ streams using remotely sensed data (Forney et al. 2013).

374 Several different methods have been utilized for measuring or predicting solar insolation on the ground.
375 Pyranometers are the most direct method for measuring insolation, capturing the solar radiation flux
376 density above a hemisphere as an electrical signal and cataloguing those signals in a datalogger (Kerr et
377 al., 1967). Once calibrated, these signals give a measure of the total direct and diffuse solar radiation
378 ~~intercepting irradiating~~ a point for a given period of time (Bode et al., 2014; Forney et al.,
379 2013; Musselman et al., 2015). While pyranometers give direct measurement of solar insolation for a
380 defined period of time, hemispherical photographs allow indirect estimation of solar insolation for any
381 point in time (Bode et al., 2014; Breshears et al., 1997; Rich et al., 1994). Plotting the path of the sun in
382 the area of sky captured by the hemispherical photograph allows for calculation of direct solar radiation
383 through identified canopy gaps, while gap fraction across the entire hemisphere allows for calculation of
384 diffuse radiation. Analysis of hemispherical photographs requires assumptions of ~~solar output extra-~~
385 ~~terrestrial solar radiation~~ and sky conditions in order to produce solar insolation estimates. Understory
386 light conditions can also be modeled by creating a three-dimensional reconstruction of a forest from
387 field-based biophysical measurements (Ameztegui et al., 2012) or terrestrial laser scanning (Ni-Meister
388 et al., 2008). ~~All g~~Ground-based measurements are limited by the time and cost required to collect data,
389 and thus solar insolation can only be calculated for relatively small spatial extents.

390 Airborne and satellite remote sensing methods provide a means for estimating solar insolation over
391 large spatial extents. Satellite-based methods utilizing passive remote sensing data can provide coarse-

392 scale estimates of solar radiation absorbed by tree canopies through radiative transfer models based on
393 spectral indices (Field et al., 1995;Asrar et al., 1992), but these methods are not suitable for fine-scale
394 application such as modeling stream temperature. Airborne lidar is the preferred method for
395 characterizing three-dimensional structure of forest canopies, and thus is also used to assess the
396 shading effect of those canopies. Below we discuss three different approaches that have been used in
397 previous studies to quantify solar insolation at ground level using aerial lidar.

398 *Raster Approaches*

399 Lidar data can be used to create raster datasets by selecting various attributes of lidar points within a
400 defined spatial neighborhood around a raster cell. One of the most common raster products for
401 assessing canopy structure is the light penetration index (LPI), the ratio of ground first return points
402 (typically less than 2 m in elevation above ground) to the total number of lidar first return points within
403 a given raster cell. This ratio has been shown to be useful for characterizing light extinction in canopies
404 according to the Beer-Lambert law (Richardson et al., 2009) and thus has been explored as a predictor of
405 understory light conditions (Musselman et al., 2013;Alexander et al., 2013;Bode et al., 2014). [Solar](#)
406 [radiation calculators in GIS software](#) ~~GIS software solar radiation calculators~~ can also be used to
407 compute solar insolation on a lidar-derived digital elevation model (DEM). Bode et al. (2014) combined a
408 ~~GRASS r.sun solar insolation estimation~~ [r.sun solar insolation model for the GRASS GIS software](#) based
409 on a DEM with LPI to produce estimates of ground level solar insolation that showed high accuracy
410 compared to pyranometer-collected field data in a mixed forest in Northern California, USA.

411 *Lidar Point Reprojection*

412 Lidar point returns can be reprojected from the X,Y,Z Cartesian coordinate system in which they are
413 most often delivered by a vendor into a spherical coordinate system which centers the point cloud
414 around a specific location on the ground. This reprojection allows for a circular graph of the lidar point

415 returns to be created around a point at ground level. Alexander et al. (2013) created a canopy closure
416 metric from these projected point graphs based on gap fraction, and found that this metric was
417 correlated to Ellenburg indicator values (which relate plants to their ecological niche along an
418 environmental gradient) of understory light availability. Moeser et al. (2014) created synthetic
419 hemispherical photographs from reprojected lidar returns, and solar irradiance at ground level was
420 calculated using traditional hemispherical photograph analysis software. The processed synthetic
421 hemispherical photographs showed good correlation to pyranometer measured solar irradiance at three
422 field sites in eastern Switzerland.

423 *Point Cloud Approaches*

424 Because lidar point clouds are typically represented in a three-dimensional Cartesian coordinate system,
425 it is possible to model the sun's position in relation to that three-dimensional space. The number of
426 lidar returns that are reflected from a defined volume between the direction of the sun and the ground
427 can then be calculated. These methods are computationally intensive, but have shown promise for
428 providing the most direct measure of understory light availability. Lee et al. (2008) calculated the
429 number of points within a conical field of view directed at the sun's location and created a model to
430 relate this to ceptometer measurements of photosynthetically active understory solar radiation at
431 specific times and locations in a pine forest in northern Florida, USA. This method is limited by its
432 reliance on raw lidar point counts specific to the actual and relative point densities within their lidar
433 acquisition. Raw point counts are affected by both changes in flight characteristics between missions,
434 and the patterns of flight line overlap within a mission. A different point cloud approach involves a linear
435 tracing of the sun's rays along their path to the ground, and Martens et al. (2000) demonstrated how a
436 ray-tracing algorithm could be used to characterize understory light conditions in a computer simulated
437 forest. Peng et al. (2014) combined a lidar-based ray tracing algorithm with field-collected canopy base

438 heights to produce an estimate of understory solar insolation based on the Beer-Lambert law that
439 compared well to field-collected pyranometer data but is limited in practical application because of its
440 reliance on field-measured data in its model. Musselman et al. (2013) used a ray-tracing algorithm to
441 produce highly detailed estimates of direct beam solar transmittance in 5-minute increments by
442 voxelizing the lidar data and summing the number of voxels that a ray intercepted between the point of
443 origin and the sun. The algorithm relied on site-specific pyranometer measurements to calibrate and
444 adjust the beam transmittance, and therefore we were restricted from testing this method in this study.

445 Our objectives were to test the accuracy and precision of established methods of quantifying solar
446 insolation from aerial lidar within areas of narrow, heavily forested streams. We utilized ~~the two~~ raster
447 approaches and ~~the one~~ lidar point reprojection approach, ~~two-three~~ methodologies that had not been
448 previously applied and tested using high quality field data collected in heavily forested streams. We
449 evaluated the ~~two-three methods-methodologies using simple linear regressions that compared lidar~~
450 ~~derived metrics to using simple linear regressions that compared lidar-derived metrics to~~ field-based
451 pyranometer measurements of solar insolation and hemispherical photograph-based measures of shade
452 in Western Oregon, USA. Further, we sought to apply this method to quantify solar insolation
453 throughout a small headwater stream network.

454

455 B. Methods

456 *Study Site*

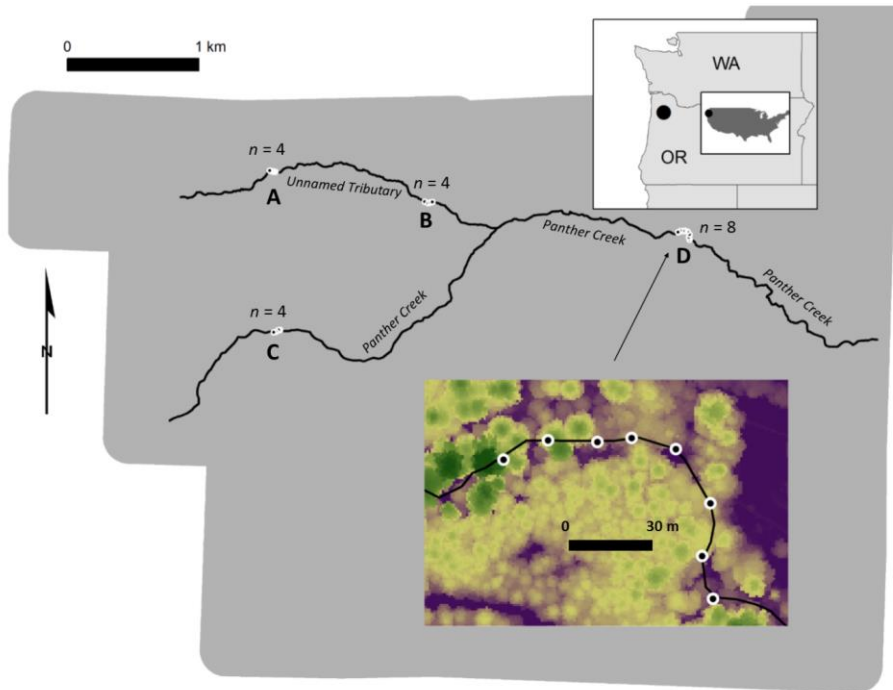
457 All field locations were located within the wetted channel of Panther Creek and a tributary (Figure 1) in
458 narrow streams (1-6 m in width) located in the east side of the Coast Range of Oregon, USA within a
459 larger research area in which lidar has been used to quantify forest canopy structure (Flewelling and
460 McFadden, 2011). All field sites were within a mature Douglas-fir (*Pseudotsuga menziesii*) forest, with

461 other dominant trees including red alder (*Alnus rubra*), Western red-cedar (*Thuja plicata*), and Western
462 hemlock (*Tsuga heterophylla*). The elevation profile and description of the stream can be found in
463 (Richardson and Moskal, 2014). The center of the channel was manually digitized as a polyline in ArcGIS
464 using a combination of aerial imagery and the vendor-provided lidar DEM.

465 Four transects were installed in late June 2015 using a Leica Builder Total Station and georeferenced
466 using a Javad Maxor GPS unit. The locations of the transects can be seen in Figure 1, with the 19 point
467 locations used for capturing field data denoted by black dots surrounded by white circles (A contains 3
468 points, B and C contain 4 points, and D contains 8 points). Transect locations were chosen manually in
469 order to maximize variability in forest shade while allowing for safe access by the field crew. Each point
470 location was located within the stream channel and marked by driving rebar into the substrate until only
471 1 m was exposed above the water surface. Point locations were approximately 15 m apart within a
472 transect in order to allow data from multiple point locations to be collected by a single datalogger.

473 Two datasets were collected at each point location during the last two weeks of June in 2015. A
474 hemispherical photograph was collected using a Nikon CoolPix 4500 digital camera leveled on a tripod 1
475 m above the ground under uniform sky condition (Figure 2) utilizing a method to find the optimum light
476 exposure (Zhang et al., 2005). Each hemispherical photograph was analyzed using the Gap Light Analyzer
477 (GLA) program (Frazer et al., 1999) in order to produce estimates of percent transmittance for diffuse
478 and direct sunlight. An Apogee Instruments SP-110 self-powered silicon-cell pyranometer, leveled and
479 mounted to the rebar pole at 1 m height (Figure 3) was used to collect a full day's solar output at each
480 point location using the datalogger. The raw voltage values collected by the datalogger were calibrated
481 to solar irradiance using the closest publicly available meteorological data. All pyranometer datasets
482 were collected on cloudless days, except for transect A, and pyranometer data from transect A was not
483 used in this study. The calibrated pyranometer data from a point location from transect D is shown in

484 Figure 4. Note that the silicon-cell photodiodes, such as the SP-110 can, produce erroneous readings
485 under conifer canopies. A black body thermopile pyranometer would have been more appropriate for
486 this study but was not available to the authors.



487
488
489 *Figure 1: Study area in northwestern Oregon (USA). The grey polygon is the extent of the 2015 lidar*
490 *acquisition. The black circles surrounded by white circles represent the 19 point locations. The letters A,*
491 *B, C, and D denote the four transects. The inset shows transect D and the background raster in the inset*
492 *is the lidar derived canopy height model with green representing tall trees and purple representing the*
493 *lowest heights. The direction of flow is from west to east.*

494



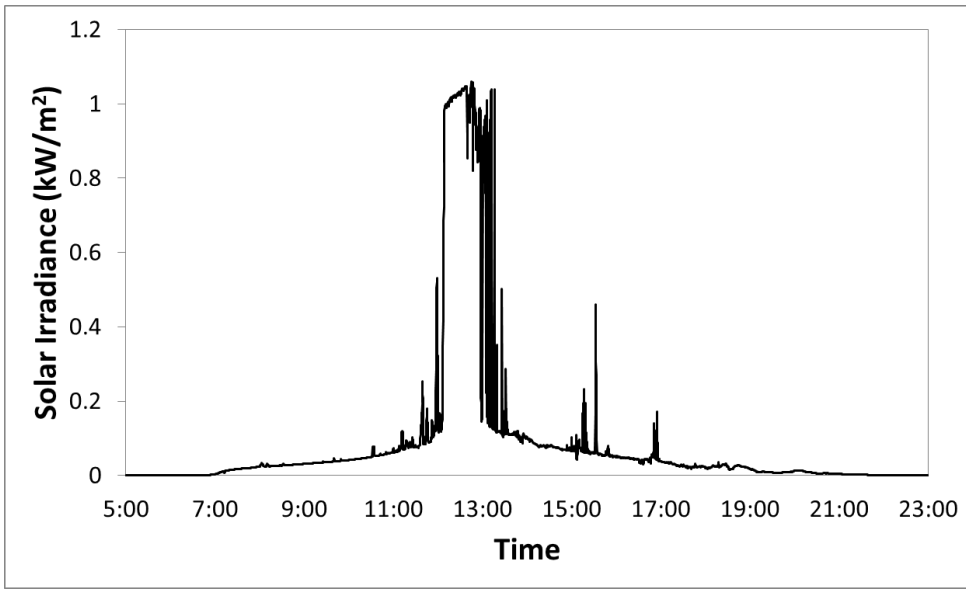
495

496 *Figure 2: Example of hemispherical photograph acquisition at a plot location in transect D.*



497

498 *Figure 3: Example of pyranometer installation at transect D (note that pyranometer is mounted on south*
499 *side of pole at a height of 1 m).*



500
501

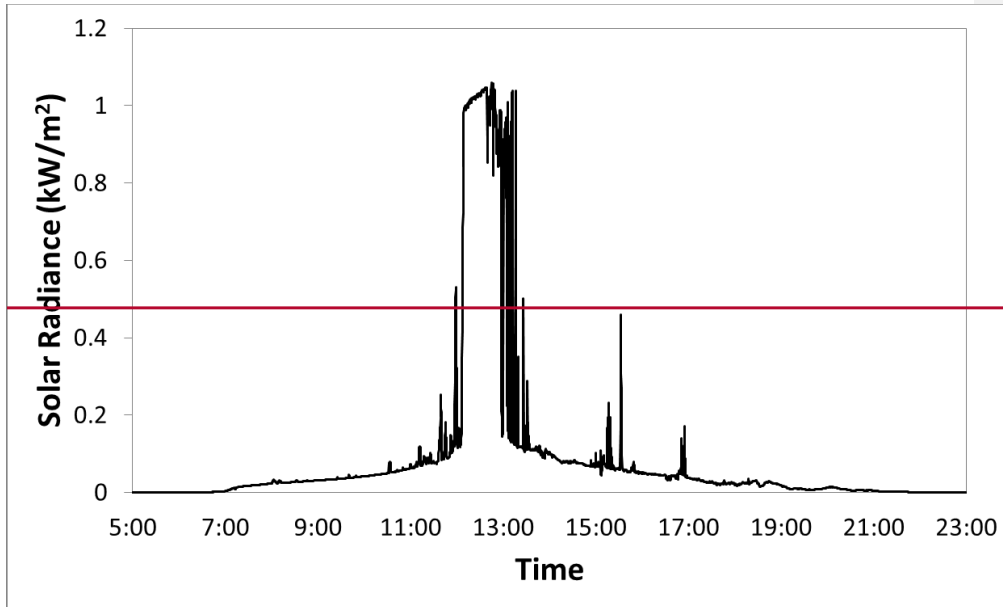


Figure 4: Daily pyranometer output from sunset to sundown for a plot in Transect D

Lidar Data and Analysis

Airborne discrete-return lidar was acquired in June of 2015 according to the specifications described in Table 1. The vendor provided processed discrete lidar point returns as well as a lidar DEM and highest hit model at a pixel resolution of 1 m. The highest hit model was subtracted from the DEM to create a canopy height model (CHM) describing the vegetation height normalized to the ground surface. In addition, Fusion (McGaughey, 2009) was used to subtract the elevations of the raw lidar points from the ground elevation in the DEM to produce a normalized point cloud dataset (NPCD). Note that the perspective of the lidar analyses is in reference to ground height while the field data were collected at 1 m above the ground. While this is a small difference, it could be a source of error in comparisons, especially at low solar angles.

515

Table 1: Lidar Data Specifications

Acquisition Date	June 18, 2015
Sensor	Leica ALS80
Survey Altitude	1,400 m
Pulse Rate	394.8 kHz
Field of View	30 degrees
Mean Pulse Density	25.35 pulses/m ²
Overlap	100% with 65% sidelap
Relative Accuracy	4 cm
Vertical Accuracy	5 cm

516

517

518 Effective Leaf Area Index (L_e) was computed using the NPCD according to the method in Richardson et
519 al. (2009):

$$520 L_e = -\frac{1}{k} \ln(R_g/R_t)$$

521 Where k is the extinction coefficient equal to 2, R_g is the number of first ground returns and R_t is the
522 number of total first returns. LPI was computed as:

$$523 LPI = (R_g/R_t)$$

524 LPI was computed in ArcGIS using a circular buffer with radius 10 m around each field point location
525 mirroring the radius used in Richardson et al. (2009) . LPI was also computed using a shifted square
526 buffer modified from the method of Bode et al. (2014) where the buffer side length (s) was calculated
527 based on:

528 $s = \frac{h}{\tan \theta}$

529 Where h is equal to the modal tree height across all our plots (34 m), and θ is equal to the maximum
530 lidar scan angle subtracted from 90° (75°), resulting in a buffer side length of 9.12 m. The square buffer
531 was shifted south to account for the seasonal solar angle in the northern hemisphere according to:

532 $shift = \left(\frac{s}{1 + \cos \sigma} \right) - s$

533 Where σ is equivalent to the solar angle at noon on the date of interest. A solar angle of 68° was used
534 in this study, resulting in a southern shift of 3.42 m. The buffer tool, zonal statistics tool, and move
535 command were used to achieve the shift in ArcGIS. We also computed topographically influenced solar
536 radiation using the lidar DEM and the solar radiation function in ArcGIS, but found that there was no
537 significant difference across the plot locations and thus did not use these results in subsequent analysis.

538 LPI and shifted LPI

Formatted: Font: Italic

539 Synthetic hemiphotos were created in Matlab using the method of Moeser et al. (2014) and analyzed for
540 diffuse and direct light transmittance in GLA. All statistical analyses were performed in R (version 3.4).

541 Longitudinal profiles of stream shading were created in ArcGIS in 1-m increments based on the
542 intersections of the stream polyline centerline with the raster output of modeled solar insolation.

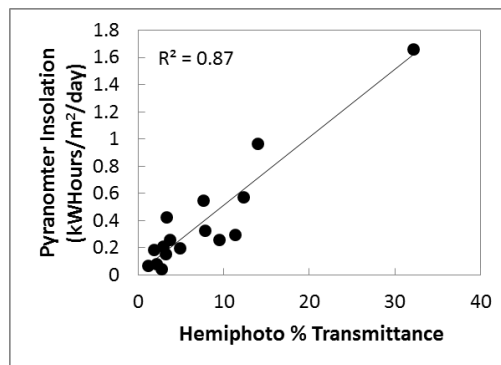
543 C. Results and Discussion

544 *Comparison between Pyranometers and Hemispherical Photographs*

545 Figure 5 shows the correlation between field-collected pyranometer data and processed hemispherical
546 photographs, with data from transect A removed. These data are highly correlated ($r^2 = 0.87$), but these
547 data are also not equally distributed across a range of solar insolation. Many more plot locations were at

548 low levels of solar insolation than in areas of relatively low shade. This is very typical of the heavily
549 forested streams in northwestern North America. Note that none of our plot locations contained
550 transmittance greater than 40%.

551



552

553 *Figure 5: Comparison between pyranometer-measured solar insolation and daily diffuse and direct radiation*
554 *canopy transmittance calculated from hemispherical photographs.*

555

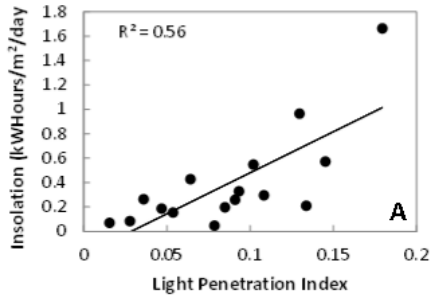
556 Model Comparisons-Linear Regressions

557 Pyranometer-based solar insolation and hemispherical photograph percent diffuse and direct radiation
558 transmittance calculated at all point locations except transect A were compared to a ~~variety-three of~~
559 lidar predictors using simple linear regression. These results are shown in Figure 6. The LPI calculated
560 using a 10 m circle centered on the point location explained about 55% of the variability in both
561 response variables, but the prediction accuracy ~~significantly~~ improved when LPI was calculated using the
562 shifted square buffer. Shifted LPI explained 74% of the variability in solar insolation and 64% of the
563 variability in percent transmittance. Synthetic hemispherical photographs explained 77% of the
564 variability in solar insolation and 60% of the variability in percent transmittance. Figure 6 shows

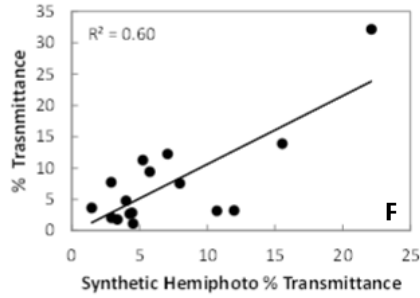
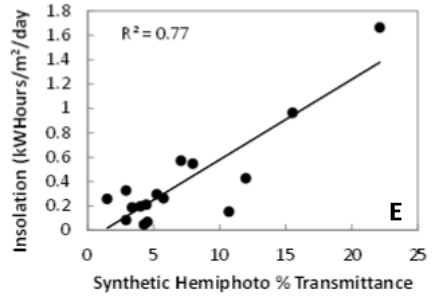
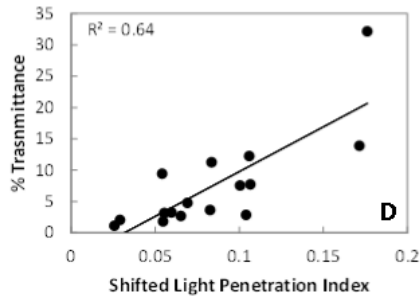
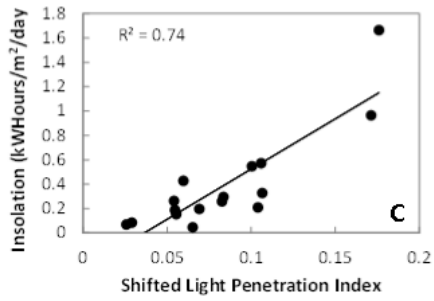
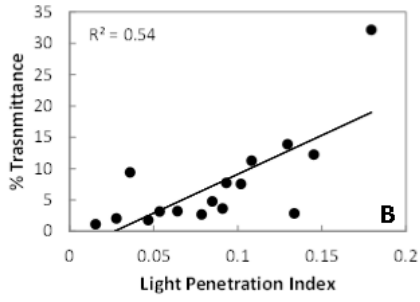
565 comparisons between transects B, C, and D to make interpretation easier, but Table 2 shows the results
566 of linear regressions between predicted variables and hemispherical photograph transmittance for all
567 plot locations resulting in small reductions in the amount of variability explained. Table 3 gives ~~model~~
568 parameters of slope and intercept resulting from the simple linear regression.

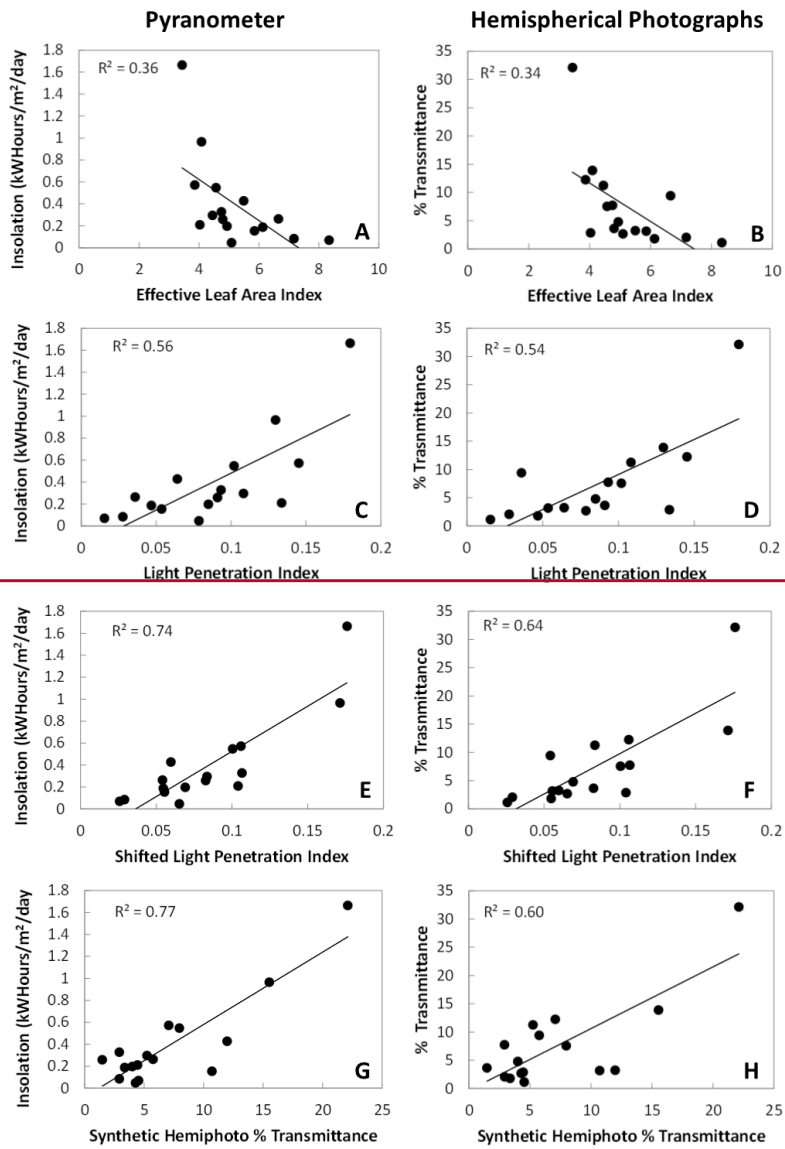
569

Pyranometer



Hemispherical Photographs





571

572

573

574

Figure 6: Simple linear regressions ~~between-between lidar~~ predictor variables and field measured pyranometer

solar insolation

(A, C, E) and hemispherical photograph % transmittance (B, D, F) omitting data from transect A

575

576

577

Table 2: Coefficients of determination for the simple linear regression between predictor variables and

578

hemispherical photograph transmittance using three additional point locations from transect A

579

Predictor Variable	Coefficient of Determination (r^2)
Light Penetration Index	0.54
Shifted Light Penetration Index	0.54
Synthetic Hemispherical Photograph % Transmittance	0.45

580

581

582

583

584

585

586

587

588

589

590

591

592

Table 3: ~~Model p~~Parameters from simple linear regressions. Note that all regressions are significant ($p < 0.05$). Data

593

from transect A are excluded.

594

Response Variable	Predictor Variable	Slope	Intercept
Hemispherical Photograph % Transmittance	Effective Leaf Area Index	-3.40	25.26
	Light Penetration Index	124.09	-3.29
	Shifted Light Penetration Index	142.2	-4.49
	Synthetic Hemispherical photograph % Transmittance	1.01	-0.32
Pyranometer Insolation	Effective Leaf Area Index	-0.19	1.37
	Light Penetration Index	6.73	-0.19
	Shifted Light Penetration Index	8.23	-0.30
	Synthetic Hemispherical Photograph % Transmittance	0.07	-0.08

595

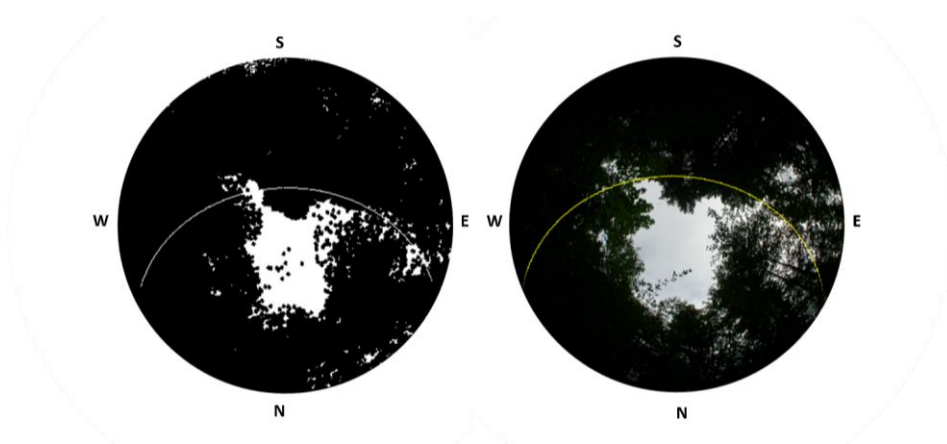
596

597 While both the raster-based shifted LPI approach and the lidar point reprojection synthetic
 598 hemispherical photograph approach explained more than 60 % of the variability in the field
 599 data achieved satisfactory model performance, the limited range of solar insolation conditions at the
 600 point locations in our study may limit some of the conclusions that can be drawn. Excluding transect A,
 601 14 of the 16 point locations received less than 0.8 kWhours/m²/day, leading to the other two point
 602 locations to exert a large degree of leverage on the ~~model~~-results. Note that these two point locations

603 ~~received less than 35% of the maximum solar insolation.~~ The three points in transect A all received less
604 than 0.8 kWh/m²/day and their inclusion in ~~Table 2 the model results (Table 2)~~ did not improve
605 ~~model results coefficients of determination,~~ suggesting that all ~~models methods~~ are not as effective at
606 predicting field measured values in areas of high canopy cover. The constraints of the study design
607 requiring point locations to be located in the stream made it impossible to achieve a greater range in
608 solar insolation. It is reasonable to expect that including more point locations receiving larger amounts
609 of insolation would have led to improved ~~model~~ accuracy and greater coefficients of determination, as
610 previous studies have shown that accuracy increases as canopy cover decreases (Moeser et al.,
611 2014; Musselman et al., 2013; Richardson and Moskal, 2014). ~~In areas with no canopy and thus no lidar~~
612 ~~point returns above the ground, the models should show better agreement with field measurements.~~
613

614 One explanation of the decrease in variability ~~explained by the models at at~~ high canopy cover ~~in~~
615 ~~regressions E and F shown in Figure 5 is~~ demonstrated in Figure 7. Here, a synthetic hemispherical
616 photograph from transect D is compared to a field-captured hemispherical photograph with the GLA
617 modeled sunpath superimposed. This sunpath is critical for determining the quantity of direct light, but
618 very small differences in the center location of the two images can produce large differences in the
619 modeled direct light. The sunpath passes through a modeled canopy gap near solar noon on the
620 synthetic hemispherical photograph, while it intersects only canopy and misses the gap on the field-
621 collected hemispherical photograph. Very small registration errors can cause ~~significant~~ differences in
622 transmittance at low light levels, and we suggest that these errors are likely to cause the errors
623 observed in the ~~models regressions.~~ The daily pyranometer output for the same point location is shown
624 in Figure 8 to further aid comparison. The pyranometer is only briefly exposed to full sunlight,
625 highlighting the contribution of small gaps in the canopy.
626

627 Understory vegetation is another likely cause of observed errors, as airborne lidar is inherently limited in
628 its ability to fully sample multi-layered canopies (Richardson and Moskal, 2011). We noticed several
629 points with ~~significant differences to the model results between lidar predictors and field data~~ that
630 contained understory vegetation in close proximity to the field instruments. The ideal scenario would be
631 for the lidar scan angles to precisely match the range of potential solar angles at each plot location, but
632 this is currently impractical, leading to an incomplete sample of the canopy light environment which
633 contributes to the ~~observed errors. errors observed in the models.~~



634
635 *Figure 7: Sunpath superimposed on a synthetic hemispherical photograph (left) and a field acquired hemispherical*
636 *photograph (right) at a point location in Transect D. The letters represent the four cardinal directions.*

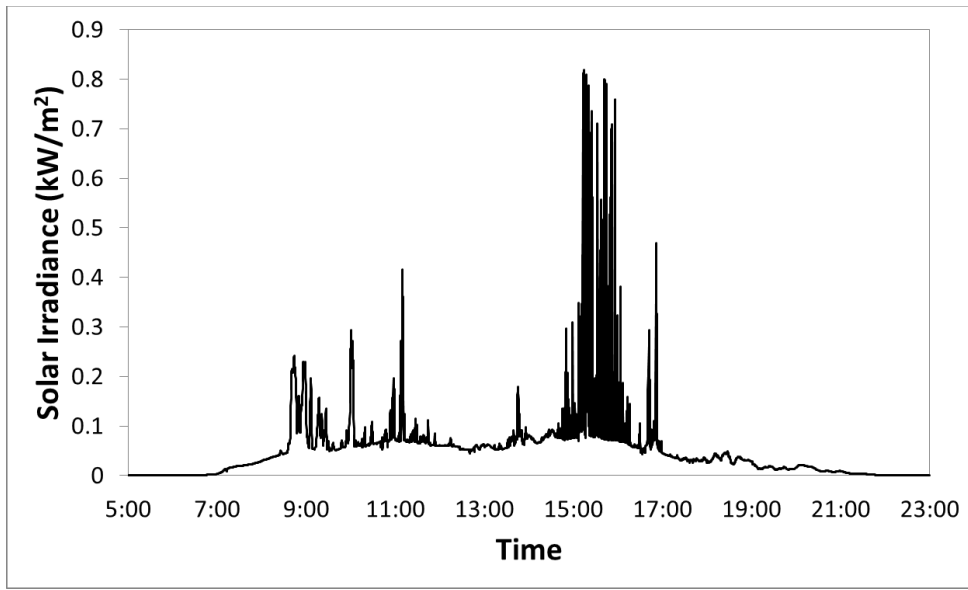


Figure 8: Daily pyranometer output from sunset to sundown for the same plot as Figure 7.

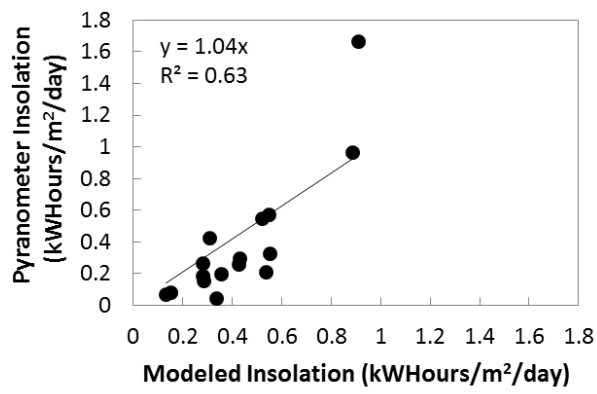
Formatted: Centered

Model Application Solar Insolation

The correlations between lidar predictors and field data were strongest in (Figure 6 C and Figure 6 E) performed the best and, and these lidar predictors are -are both appropriate to use as the basis for estimating solar insolation across the study area. Implementation of Model G-shifted LPI was the simplest and least time-intensive method, and we chose to model solar radiation -modify Model G by multiplying shifted LPI by the maximum above canopy solar insolation for June 20, 2015 and then computing a non-intercept linear regression ((Figure 98). Removing the intercept from the model lowered the coefficient of determination but provided a model with very little bias, only slightly underestimating model insolation that did not estimate negative values of solar insolation. Figure 109 shows the model applied across the study area. The graphs show the pattern of solar insolation across

Formatted: Font: Italic

651 the two reaches in the study, highlighting the utility of these methods for predicting solar insolation in
652 heavily forested streams across wide spatial extents. Figure 11e shows the relative frequency of binned
653 solar insolation values, highlighting the dominance of heavily shaded areas (note that a dammed
654 reservoir, point D on the map, contributes the majority of the points in full sun).
655



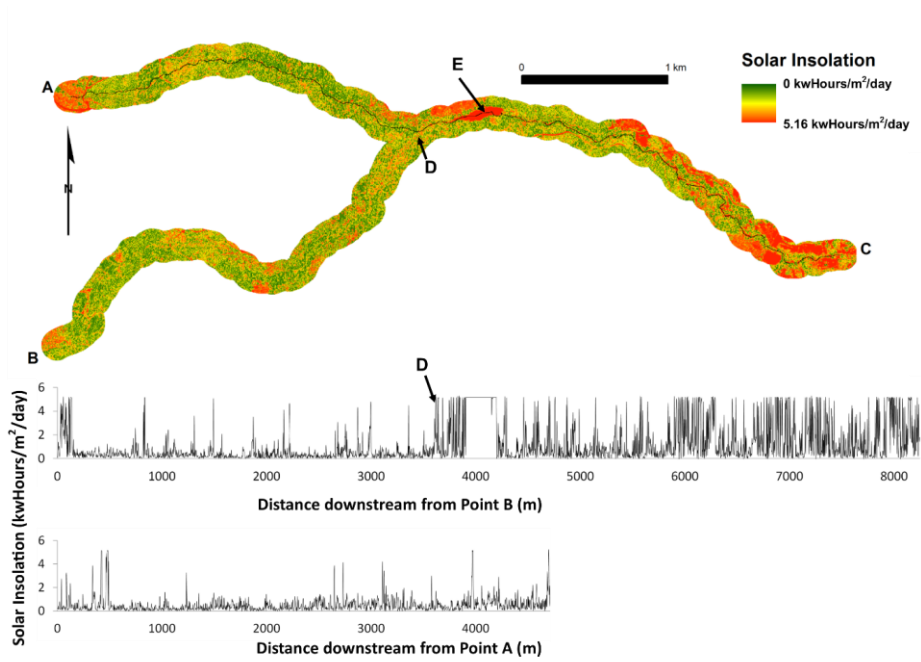
656

657 *Figure 89:* Model used for generation of landscape scale solar insolation estimates

658

659

660

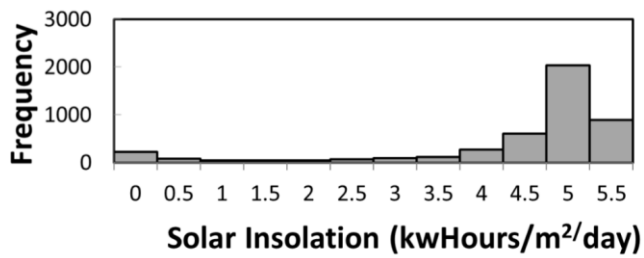


661

662

663 *Figure 109: Map of model derived solar insolation for Panther Creek (top) and graph of model derived*
 664 *solar insolation for reach A-C (middle) and reach B-D (bottom). Point E is a dammed reservoir. Note the*
 665 *direction of flow is toward point C*

666



667

668 *Figure 114: Histogram of solar insolation pixel values along reach A-C from Figure 9*

669

670 The relatively unbiased results shown in Figure 98 show that field calibration is not required to produce
671 accurate estimates of solar insolation. However, information is still needed on local above-canopy
672 meteorological conditions, which can either be modeled from known solar outputs or collected from a
673 nearby meteorological station. Little bias was observed in comparisons between synthetic
674 hemispherical photograph transmittance and field-based hemispherical photograph transmittance
675 (Table 3). Therefore, both approaches tested in this study should not require field calibration.

676

677 D. Conclusions

678 We tested two approaches for estimating solar insolation from airborne lidar using field data collected
679 in a heavily forested narrow stream, showing that an LPI-based raster approach and a synthetic
680 hemispherical photograph approach ~~can accurately~~ predict solar insolation and light transmittance.
681 These results should be interpreted with the caveat that our point locations contained few areas with
682 high insolation. We showed that the LPI-based model can be applied across the landscape, and we
683 demonstrated that no field-based calibration was necessary to produce unbiased prediction of solar
684 insolation.

685 This study lays the groundwork for additional research on remote sensing methods for quantifying light
686 conditions in riparian areas over heavily forested streams. ~~First, point cloud based approaches utilizing
687 ray tracing need to be further developed. The results of this study suggest that refined ray tracing
688 approaches should not require calibration. Ray tracing is perhaps the most elegant method for
689 accurately modeling the relationship between lidar points and the sun, but this method requires a large
690 amount of computational power to model multiple sun angles for each lidar point. One method that we
691 were unable to test is ray-tracing and future research should continue to develop this approach.~~ Second,

692 research should focus on exploring the limit of matching ground-based measurements to lidar-predicted
693 solar insolation. Lastly, the limitation of aerial lidar to quantify understory light conditions in multi-
694 layered canopies should be explored in more detail to better understand when and if airborne sensors
695 are inappropriate for these particular applications. In these circumstances, other sensors such as
696 terrestrial lidar or ground-based digital photographs utilizing structure from motion may provide
697 additional useful information.

698 E. Data availability

699 The GPS data, pyranometer data, processed hemispherical photograph data, spreadsheets used for data
700 analysis, and access to the LiDAR data can be found at <https://doi.org/10.17632/vwmxw4hcj7.1>

701 F. Acknowledgements

702 We are grateful to Dave Moeser for sharing his MATLAB code for creating synthetic hemispherical
703 photographs and to Keith Musselman for advising on the applicability of ray-tracing methods. Guang
704 Zheng also assisted with research into ray-tracing methods. Caileigh Shoot and Natalie Gray coordinated
705 field data collection. This work was supported by the Precision Forestry Cooperative, the Bureau of Land
706 Management, and the U.S. Geological Survey. Any use of trade, product or firm names is for descriptive
707 purposes only and does not imply endorsement by the U.S. government.

708 G. References

709 Alexander, C., Moeslund, J. E., Bocher, P. K., Arge, L., and Svenning, J. C.: Airborne laser scanner (LiDAR)
710 proxies for understory light conditions, *Remote Sensing of Environment*, 134, 152-161,
711 10.1016/j.rse.2013.02.028, 2013.

712 Ameztegui, A., Coll, L., Benavides, R., Valladares, F., and Paquette, A.: Understory light predictions in
713 mixed conifer mountain forests: Role of aspect-induced variation in crown geometry and openness,
714 Forest Ecology and Management, 276, 52-61, <http://dx.doi.org/10.1016/j.foreco.2012.03.021>, 2012.

715 Asrar, G., Myneni, R. B., and Choudhury, B. J.: Spatial heterogeneity in vegetation canopies and remote
716 sensing of absorbed photosynthetically active radiation: A modeling study, Remote Sensing of
717 Environment, 41, 85-103, [http://dx.doi.org/10.1016/0034-4257\(92\)90070-Z](http://dx.doi.org/10.1016/0034-4257(92)90070-Z), 1992.

718 Bode, C. A., Limm, M. P., Power, M. E., and Finlay, J. C.: Subcanopy Solar Radiation model: Predicting
719 solar radiation across a heavily vegetated landscape using LiDAR and GIS solar radiation models, Remote
720 Sensing of Environment, 154, 387-397, <http://dx.doi.org/10.1016/j.rse.2014.01.028>, 2014.

721 Breshears, D. D., Rich, P. M., Barnes, F. J., and Campbell, K.: Overstory-imposed heterogeneity in solar
722 radiation and soil moisture in a semiarid woodland, Ecol. Appl., 7, 1201-1215, 10.1890/1051-
723 0761(1997)007[1201:OIHISR]2.0.CO;2, 1997.

724 Field, C. B., Randerson, J. T., and Malmström, C. M.: Global net primary production: Combining ecology
725 and remote sensing, Remote Sensing of Environment, 51, 74-88, [http://dx.doi.org/10.1016/0034-4257\(94\)00066-V](http://dx.doi.org/10.1016/0034-4257(94)00066-V), 1995.

727 Flewelling, J. W., and McFadden, G.: LiDAR data and cooperative research at Panther Creek, Oregon,
728 SilviLaser, Hobart, Australia, October 16-20, 2011, 2011.

729 Forney, W. M., Soulard, C. E., and Chickadel, C. C.: Salmonids, stream temperatures, and solar loading—
730 modeling the shade provided to the Klamath River by vegetation and geomorphology, 25, 2013.

731 Frazer, G. W., Canham, C. D., and Lertzman, K. P.: Gap Light Analyzer (GLA), Version 2.0, in, Simon Fraser
732 University, Burnaby, British Columbia, 1999.

733 Hock, R.: Temperature index melt modelling in mountain areas, Journal of Hydrology, 282, 104-115,
734 [http://dx.doi.org/10.1016/S0022-1694\(03\)00257-9](http://dx.doi.org/10.1016/S0022-1694(03)00257-9), 2003.

735 Holtby, L. B.: Effects of logging on stream temperatures in Carnation Creek British Columbia, and
736 associated impacts on the coho salmon (*Oncorhynchus kisutch*), Canadian Journal of Fisheries and
737 Aquatic Sciences, 45, 502-515, 10.1139/f88-060, 1988.

738 Kerr, J. P., Thurtell, G. W., and Tanner, C. B.: An integrating pyranometer for climatological observer
739 stations and mesoscale networks, Journal of Applied Meteorology, 6, 688-694, 10.1175/1520-
740 0450(1967)006<0688:AIPFCO>2.0.CO;2, 1967.

741 Lee, H., Slatton, K. C., Roth, B. E., and Cropper, W. P.: Prediction of forest canopy light interception using
742 three-dimensional airborne LiDAR data, International Journal of Remote Sensing, 30, 189-207,
743 10.1080/01431160802261171, 2008.

744 Leinenbach, P., McFadden, G., and Torgersen, C. E.: Effects of riparian management strategies on stream
745 temperature, 22, 2013.

746 Martens, S. N., Breshears, D. D., and Meyer, C. W.: Spatial distributions of understory light along the
747 grassland/forest continuum: effects of cover, height, and spatial pattern of tree canopies, Ecological
748 Modelling, 126, 79-93, [http://dx.doi.org/10.1016/S0304-3800\(99\)00188-X](http://dx.doi.org/10.1016/S0304-3800(99)00188-X), 2000.

749 McGaughey, R. J.: FUSION/LDV: software for LIDAR data analysis and visualization, 2.51 ed., United
750 States Department of Agriculture, Forest Service, Pacific Northwest Research Station, 2009.

751 Moeser, D., Roubinek, J., Schleppi, P., Morsdorf, F., and Jonas, T.: Canopy closure, LAI and radiation
752 transfer from airborne LiDAR synthetic images, Agricultural and Forest Meteorology, 197, 158-168,
753 10.1016/j.agrformet.2014.06.008, 2014.

754 Moore, R. D., Spittlehouse, D. L., and Story, A.: Riparian microclimate and stream temperature response
755 to forest harvesting: a review, JAWRA Journal of the American Water Resources Association, 41, 813-
756 834, 10.1111/j.1752-1688.2005.tb03772.x, 2005a.

757 Moore, R. D., Sutherland, P., Gomi, T., and Dhakal, A.: Thermal regime of a headwater stream within a
758 clear-cut, coastal British Columbia, Canada, Hydrol. Process., 19, 2591-2608, 10.1002/hyp.5733, 2005b.

759 Musselman, K. N., Margulis, S. A., and Molotch, N. P.: Estimation of solar direct beam transmittance of
760 conifer canopies from airborne LiDAR, *Remote Sensing of Environment*, 136, 402-415,
761 <http://dx.doi.org/10.1016/j.rse.2013.05.021>, 2013.

762 Musselman, K. N., Pomeroy, J. W., and Link, T. E.: Variability in shortwave irradiance caused by forest
763 gaps: measurements, modelling, and implications for snow energetics, *Agricultural and Forest*
764 *Meteorology*, 207, 69-82, 10.1016/j.agrformet.2015.03.014, 2015.

765 Ni-Meister, W., Strahler, A. H., Woodcock, C. E., Schaaf, C. B., Jupp, D. L. B., Yao, T., Zhao, F., and Yang,
766 X.: Modeling the hemispherical scanning, below-canopy lidar and vegetation structure characteristics
767 with a geometric-optical and radiative-transfer model, *Canadian Journal of Remote Sensing*, 34, S385-
768 S397, 10.5589/m08-047, 2008.

769 Nicotra, A. B., Chazdon, R. L., and Iriarte, S. V. B.: Spatial heterogeneity of light and woody seedling
770 regeneration in tropical wet forests, *Ecology*, 80, 1908-1926, 10.1890/0012-
771 9658(1999)080[1908:SHOLAW]2.0.CO;2, 1999.

772 Peng, S. Z., Zhao, C. Y., and Xu, Z. L.: Modeling spatiotemporal patterns of understory light intensity
773 using airborne laser scanner (LiDAR), *ISPRS-J. Photogramm. Remote Sens.*, 97, 195-203,
774 10.1016/j.isprsjprs.2014.09.003, 2014.

775 Rich, P., Dubayah, R., Hetrick, W., and Saving, S.: Using viewshed models to calculate intercepted solar
776 radiation: applications in ecology. *American Society for Photogrammetry and Remote Sensing Technical*
777 *Papers*, American Society of Photogrammetry and Remote Sensing, 1994, 524-529,

778 Richardson, J. J., Moskal, L. M., and Kim, S.-H.: Modeling approaches to estimate effective leaf area
779 index from aerial discrete-return LIDAR, *Agricultural and Forest Meteorology*, 149, 1152-1160,
780 10.1016/j.agrformet.2009.02.007, 2009.

781 Richardson, J. J., and Moskal, L. M.: Strengths and limitations of assessing forest density and spatial
782 configuration with aerial LiDAR, *Remote Sensing of Environment*, 115, 2640-2651,
783 10.1016/j.rse.2011.05.020, 2011.

784 Richardson, J. J., and Moskal, L. M.: Assessing the utility of green LiDAR for characterizing bathymetry of
785 heavily forested narrow streams, *Remote Sensing Letters*, 5, 352-357, 10.1080/2150704X.2014.902545,
786 2014.

787 Torgersen, C. E., Hockman-Wert, D. P., Bateman, D. S., Leer, D. W., and Gresswell, R. E.: Longitudinal
788 patterns of fish assemblages, aquatic habitat, and water temperature in the Lower Crooked River,
789 *Oregon*, 37, 2007.

790 Torgersen, C. E., Ebersole, J. L., and Keenan, D. M.: Primer for identifying cold-water refuges to protect
791 and restore thermal diversity in riverine landscapes, Seattle, WA, 91, 2012.

792 Zhang, Y. Q., Chen, J. M., and Miller, J. R.: Determining digital hemispherical photograph exposure for
793 leaf area index estimation, *Agricultural and Forest Meteorology*, 133, 166-181, 2005.

794